Inorg. Chem. **2007**, *46*, 2237–2242

$AeMg_5In_3$ (Ae = Ba, Sr): New Intermetallic Compounds with Well-Differentiated Roles for the Normal Cation Types†

Bin Li and John D. Corbett*

Ames Laboratory—DOE and Department of Chemistry, Iowa State University, Ames, Iowa 50011

Received November 9, 2006

The isostructural phases $BaMg_{4.787(3)}In_{3.213}$ and $SrMg_{4.837(2)}In_{3.163}$ were synthesized via high-temperature reactions of the elements in welded Ta tubes. The orthorhombic crystal structure established for these by single-crystal X-ray diffraction means (space group *Pnma*, $Z = 4$) features a 3D Mg–In network formed from condensed 21-vertex polyhedra that are centered by Ba (Sr), viz., $Ae@Mg_5M_7In_9$ (M = Mg/In). Three of eight independent network sites are co-occupied by >90% Mg and <10% In(M). The network structure is the inverse of that found in the isopointal $Ca(CaIn_4)Au_3$, as clearly delineated by site charge estimates for the equivalent In_3 versus Au_3 positions. Tight-binding LMTO and extended Hückel calculations on the ordered $AeMg_5In_3$ support the differentiation of Mg and Ae in the structure, with substantial participation of Mg in dominant Mg–In bonding, but mainly an electron donor role for Ae. The Fermi energies lie close to pseudo gaps but with substantial DOS remaining, consistent with their measured metallic properties. An unmixed ideal $AeMg_5In_3$ would be isostructural with YCo_5P_3, with comparable polyhedra, but the small P in the latter lacks an effective interbridging role.

Introduction

Owing to the pronounced differences in electronegativities between alkaline-earth and post-transition metals, the alkaline-earth metals in their binary or higher compounds appear to act mainly as "spacers" and electron donors encapsulated in anionic networks.[1] Phases such as $SrIn_4$ and Sr_3In_5 have also revealed the importance of relative cation sizes in determining the nature of the network substructure of the indides.[2] The bonding in these phases is generally characterized in terms of greater covalent interactions within the anionic part of the structures rather than in terms of strong cation−anion covalence. Good examples are $Ca_{31}Sn_{20}$,[3] $Na_{10}AeSn_{12}$ (Ae = Ca, Sr),[4] and Na_8BaSn_6[5] with measured semiconductor properties, consistent with their structure−property relationships when both alkali and alkaline-earth metal atoms are treated as electron donors to the Sn substructures. Magnesium atoms also appear to act as spacers in some compounds, as in Mg_2Zn_{11},[6] $Mg_2Cu_6M_5$ (M = Al, Ga),[7] and $Mg_{35}Cu_{24}Ga_{53}$.[8]

However, our recent research in alkali-metal−Mg−In systems have shown that magnesium may often bond within anionic clusters along with indium rather than fill space within or between polyanions. For example, triply fused icosahedra M_{28} polyhedra (M = In/Mg) and pentacapped trigonal prismatic clusters M_{11} occur in $K_{34}Mg_{13.95}In_{91.05(9)}$[9] and $Rb_{14}Mg_{4.5}In_{25.5}$,[10] respectively. In both structures, all of the Mg mixes with indium in the indium substructure; that is, there are no independent Mg sites. Site mixing of Mg and In is also found in the new structure $(Mg,In)_3Ir$.[11] Related chemistry also occurs with Li instead of Mg, as in $K_{34}In_{92.30(7)}Li_{12.70(7)}$ and $K_{14}Na_{20}In_{91.82(8)}Li_{13.18(8)}$.[12] Recently, we discovered another variation in $K_3Mg_{20}In_{14}$[13] in which all of the Mg and In sites are independent, but they still define a 3D

† This research was supported by the Office of the Basic Energy Sciences, Materials Sciences Division, U. S. Department of Energy (DOE). The Ames Laboratory is operated for the DOE by Iowa State University under contract no. W-7405-Eng-82.

* To whom correspondence should be addressed. E-mail: jcorbett@iastate.edu.

(1) (a) Corbett, J. D. In *Chemistry, Structure, and Bonding of Zintl Phases and Ions*; Kauzlarich S., Ed.; VCH Publishers: New York, 1996; Chapter 3; (b) Corbett, J. D. *Angew. Chem., Int. Ed.* **2000**, *39*, 670.
(2) (a) Seo, D.-K.; Corbett, J. D. *J. Am. Chem. Soc.* **2000**, *122*, 9621; (b) Seo, D.-K.; Corbett, J. D. *J. Am. Chem. Soc.* **2001**, *123*, 4512.
(3) Ganguli, A. K.; Guloy, A. M.; Leon-Escamilla, E. A.; Corbett, J. D. *Inorg. Chem.* **1993**, *32*, 4349.
(4) Bobev, S.; Sevov, S. C. *Inorg. Chem.* **2001**, *40*, 5361.
(5) Todorov, L.; Sevov, S. C. *Inorg. Chem.* **2004**, *43*, 6490.
(6) Samson, S. *Acta Chem. Scand.* **1949**, *3*, 835.
(7) (a) Lin, Q.; Corbett, J. D. *Inorg. Chem.* **2003**, *42*, 8762. (b) Samson, S. *Acta Chem. Scand.* **1949**, *3*, 809.
(8) Lin, Q.; Corbett, J. D. *Inorg. Chem.* **2005**, *44*, 512.
(9) Li, B.; Corbett, J. D. *Inorg. Chem.* **2006**, *45*, 8958.
(10) Li, B.; Corbett, J. D. *Inorg. Chem.* **2006**, *45*, 156.
(11) Hlukhyy, V.; Hoffmann, R. D.; Pöttgen, R. *Z. Anorg. Allg. Chem.* **2004**, *630*, 68.
(12) Li, B.; Corbett, J. D. *J. Am. Chem. Soc.* **2005**, *127*, 926.
(13) Li, B.; Corbett, J. D. *Inorg. Chem.* **2006**, *45*, 3861.

10.1021/ic0621289 CCC: $37.00 © 2007 American Chemical Society
Published on Web 02/20/2007

Mg−In network with substantial Mg participation in the overall network bonding. The special role of magnesium in the alkali-metal−Mg−In systems, acting as part of an anionic network instead of as an electron donor and space-filler, has motivated us to study differentiated roles for magnesium in alkaline-earth-metal−Mg−In systems in which no ternary compound has been reported. We report two new isostructural compounds, $BaMg_{4.787(3)}In_{3.213}$ and $SrMg_{4.837(2)}In_{3.163}$ (abbreviated as $AeMg_5In_3$), which contain both independent Mg sites and those mixed with some In, the Ae being simply encapsulated in the anionic networks.

Experimental Section

Syntheses. All of the materials were handled in N_2-filled gloveboxes with moisture levels below 1 ppm (vol). Both $AeMg_5In_3$ (Ae = Ba, Sr) were synthesized via high-temperature reactions of the elements (99.9% barium, 99.95% strontium, 99.98% magnesium, and 99.999% indium, all from Alfa-Aesar). The weighed elements were enclosed in welded tantalum tubes that were sealed in evacuated, fused silica jackets by methods and techniques described previously.[14] Single crystals of $AeMg_5In_3$ were first obtained from reaction compositions $K_{1.5}Ae_{1.5}Mg_{20}In_{14}$ that were designed to gain isostructural versions of the metallic $K_3Mg_{20}In_{14}$,[13] which is a stuffed variant of $BaHg_{11}$ and isotypic with $M_3Au_{6+x}Al_{26}Ti$ (M = Ca, Sr, Yb).[15]

Both structures were refined in space group *Pnma* (No. 62, $Z = 4$) with three of nine atom sites co-occupied by Mg and In. Once the stoichiometries had been established by crystallography, pure phases (>95%) of both compounds were synthesized directly from the appropriate compositions (judging from comparisons of their Guinier powder patterns with those calculated from the refined structures). Though both compounds exhibit mixing of In and Mg, no significant variability in these proportions was indicated by shifts of cell parameters for samples loaded with different proportions, as judged from both single crystal and powder pattern refinements. Considering that all three co-occupied positions contain more than 90% Mg, we also attempted to synthesize $BaMg_5In_3$ with all three positions fully occupied with Mg, but the main product phase is still $BaMg_{4.8}In_{3.2}$ according to the same criteria (~85% yield plus some unknown peaks). In Mg-poorer, In-richer systems, a ternary $BaAl_4$-type phase forms with both cations. Both compounds were obtained from samples heated at 1000 °C for 3 h, cooled at 10 °C/h to 500 °C, held there for 160 h to grow crystals, followed by cooling to room temperature at 5 °C/h. Both are silvery, brittle, and very sensitive to moisture or air at room temperature.

X-ray Studies. Powder diffraction data were collected with the aid of a Huber 670 Guinier powder camera equipped with an area detector and Cu Kα radiation ($\lambda = 1.540598$ Å). Powdered samples were homogeneously dispersed between two layers of Mylar with the aid of a little vacuum grease. Peak search, indexing, and least-squares refinement for cell parameters were done with the WinXPOW program.[16] Single crystals were selected from the products in a glovebox and sealed in capillaries. Single-crystal diffraction data were collected at 293 K with Mo Kα radiation on a Bruker SMART APEX CCD diffractometer and in the form of three sets of 606 frames with 0.3° scans in ω and exposure times of 10 s per frame. The 2θ range extended from ~3° to ~57°. The unit cell parameters for each were determined from data for about 900 indexed reflections. The reflection intensities were integrated with the SAINT subprogram in the SMART software package.[17] The data were corrected for Lorentz and polarization effects and for absorption empirically according to the program SADABS.[18]

Both structural solutions were obtained by direct methods and refined by full-matrix least-squares refinement on F_o^2 using the Bruker SHELXTL 6.1 software package.[19] The systematic absences in both data sets indicated their structures are primitive with possible space groups of $Pn2_1a$ (No. 33) or the centric *Pnma* (No. 62). The intensity statistics showed a clear indication of a centrosymmetric space group, and the latter group gave satisfactory refinement results. For the barium compound, direct methods provided nine peaks, of which one was assigned to Ba, three to In, and five to Mg atoms, according to peak heights. A few least-squares cycles followed by a difference Fourier map revealed that Mg alone was too electron-poor for three sites, according to their abnormally small displacement parameters and refined occupancies (>100%). At this point, $R1$ and the highest difference peak were 0.041 and 2.17 e/Å^3, respectively. Allowing mixtures of magnesium and indium at the three Mg sites gave more reasonable isotropic displacement parameters as well as improved $R1$ (0.030) and residual (2.0 e/Å^3). The refinement, finally with anisotropic displacement parameters and a secondary extinction correction, converged at R1 = 0.021, and wR2 = 0.046 ($I > 2\sigma(I)$).

The structure of the Sr compound was similarly solved and refined. From the simple viewpoint of crystallography, the three mixed Mg/In sites could also be refined as mixtures of Mg with Ba or Sr, giving different refinement compositions ($Ba_{1.18}Mg_{4.82}In_3$ and $Sr_{1.26}Mg_{4.74}In_3$) or with partially occupied indium ($BaMg_2In_{3.87}$ and $SrMg_2In_{3.84}$). Attempts to define the compositions for both compounds from EDS (energy-dispersive spectroscopy) analyses failed, probably because they are very sensitive to traces of moisture and air (for example, the samples cannot be polished before analysis). Fortunately, among the products that were obtained from reactions with all of the possible refined compositions, only the reported compositions gave pure phases according to their powder X-ray patterns. For example, the powder pattern from the loaded composition $Ba_{1.18}Mg_{4.82}In_3$ (mixing Mg and Ba) only shows ~80% of the title compound plus some unassigned peaks. The chemical and volume logic of these alternate models are, of course, also seriously lacking. The analogous Sr reaction at the corresponding alternate (Mg + Ba) composition also yielded a second, slightly different but still unidentified pattern.

The crystallographic and refinement parameters for both compounds are given in Table 1. Table 2 gives the corresponding atomic positional, isotropic-equivalent displacement parameters, and site occupancies. Table 3 contains the important interatom distances for both compounds. More detailed crystallographic and refinement data and the anisotropic displacement parameters for the reported solutions are available in the Supporting Information (cif).

Physical Property Measurements. Electrical resistivities were measured by the electrodeless "Q" method with the aid of a Hewlett-Packard 4342A Q meter.[20] The method is particularly suitable for measurements on highly air-sensitive samples. For this purpose, powdered $BaMg_{4.787(3)}In_{3.213}$ (102 mg) and $SrMg_{4.837(2)}In_{3.163}$ (109 mg) with grain diameters between 150 and 250 μm were each dispersed with chromatographic alumina and sealed into Pyrex tubes. Measurements were made at 34 MHz over the range of about

(14) Dong, Z.-C.; Corbett, J. D. *J. Am. Chem. Soc.* **1993**, *115*, 11299.
(15) Latturner, S. E.; Kanatzidis, M. G. *Inorg. Chem.* **2004**, *43*, 2.
(16) *STOE WinXPOW*, version 2.10; STOE & Cie GmbH, Hilpertst.: Darmstadt, Germany, 2004.
(17) *SMART*, Bruker AXS, Inc.; Madison, WI, 1996.
(18) Blessing, R. H. *Acta Crystallogr.* **1995**, *A51*, 33.
(19) *SHELXTL*, Bruker AXS, Inc.; Madison, WI, 2000.
(20) Zhao, J. T.; Corbett, J. D. *Inorg. Chem.* **1995**, *34*, 378.

Table 1. Crystal and Refinement Data for $BaMg_{4.787(3)}In_{3.213}$ (**I**) and $SrMg_{4.837(2)}In_{3.163}$ (**II**)

compounds	I	II
fw	622.8	568.6
space group, *Z*	*Pnma* (No. 62), 4	
unit cell (Å), *a*	14.325(1)	14.223(1)
b	4.8191(4)	4.7485(3)
c	13.687(1)	13.5929(9)
V (Å^3)	944.8 (1)	918.0(1)
d_{calcd} (g/cm^3)	4.38	4.11
μ, mm^{-1} (Mo Kα)	12.0	13.86
data/restraints/para.	1282/0/59	1236/0/59
GOF on F^2	1.115	1.172
R1/wR2 [I > 2σ(I)]	0.0211/0.0462	0.0201/0.0379
R1/wR2 (all data)	0.0228/0.0470	0.0215/0.0382
largest diff. peak and hole (e·Å^{-3})	1.05, −1.33	0.83, −1.38

Table 2. Atomic Coordinates,[a] Isotropic-Equivalent Displacement Parameters (Å^2 × 10^3), and Site Occupancies[b] for $BaMg_{4.787(3)}In_{3.213}$ and $SrMg_{4.837(2)}In_{3.163}$[c]

	x	*z*	U(eq)	Mg fraction
Ae	0.3029(1)	0.3839(1)	16(1)	
	0.3042(1)	0.3827(1)	21(1)	
In1	0.3879(1)	0.8804(1)	17(1)	
	0.3827(1)	0.8812(1)	17(1)	
In2	0.1303(1)	0.0721(1)	17(1)	
	0.1363(1)	0.0665(1)	16(1)	
In3	0.0915(1)	0.7146(1)	17(1)	
	0.0886(1)	0.7187(1)	16(1)	
M1	0.4966(1)	0.5900(1)	17(1)	0.911(3)
	0.4945(1)	0.5870(1)	19(1)	0.927(2)
M2	0.3342(1)	0.0983(1)	20(1)	0.920(3)
	0.3382(1)	0.1023(1)	20(1)	0.940(2)
M3	0.0662(1)	0.4961(1)	19(1)	0.956(3)
	0.0666(1)	0.4974(1)	20(1)	0.968(2)
Mg1	0.2982(1)	0.6824(1)	17(1)	
	0.2946(1)	0.6817(1)	18(1)	
Mg2	0.0393(1)	0.2637(1)	21(1)	
	0.0442(1)	0.2599(1)	21(1)	

[a] All atoms are in 4*c* sites with $y = {}^1/_4$. [b] M sites were assumed to be fully occupied by Mg and In, with the Mg fractions listed. [c] Values for $SrMg_{4.837(2)}In_{3.163}$ are shown on the second line.

Table 3. Selected Bond Lengths (Å) for $BaMg_{4.787(3)}In_{3.213(3)}$ (**I**) and $SrMg_{4.837(2)}In_{3.163(2)}$(**II**)

bond	I	II	bond	I	II
Ae−In1[a]	3.6442(4)	3.5647(4)	In3−M1	3.001(1)	2.961(1)
Ae−In2[a]	3.6540(4)	3.5485(4)	In3−M3	3.014(2)	3.024(2)
Ae−In3[a]	3.6688(4)	3.5958(4)	In3−M2[a]	3.0771(9)	3.0376(9)
Ae−M3	3.720(2)	3.721(2)	In3−Mg1	2.994(2)	2.973(2)
Ae−M1[a]	3.764(1)	3.743(1)	M1−M1[a]	3.444(2)	3.354(2)
In1−Mg1	2.996(2)	2.987(2)	M1−Mg1	3.111(2)	3.121(2)
In1−Mg2[a]	3.073(1)	3.072(1)	M2−M3	3.130(1)	3.082(1)
In1−M3	3.066(2)	3.093(2)	M2−M3	3.568(2)	3.520(2)
In1−M3[a]	2.9563(9)	2.941(9)	M2−M3[a]	3.072(2)	3.039(2)
In1−M2	3.081(1)	3.071(1)	M2−Mg2[a]	3.202(2)	3.244(2)
In1−In3	3.1940(5)	3.2281(5)	Mg2−In3[a]	3.067(1)	3.048(1)
In2−M1	2.928(1)	2.901(1)	Mg2−M1[a]	3.427(2)	3.3867(2)
In2−Mg2	2.930(2)	2.938(2)	Mg2−M2	3.492(2)	3.477(2)
In2−Mg1[a]	3.0245(1)	3.010(1)	Mg1−M2[a]	3.276(2)	3.221(1)
In2−M2	2.943(1)	2.913(1)	Mg1−Mg2[a]	3.530(3)	3.467(2)
In2−M1[a]	3.0292(8)	3.0283(8)			

[a] Bonds between layers in Figure 2.

95−240 K. The measured resistivities increase linearly over the range for both compounds, which is taken as the defining characteristic of a metal. The extrapolated ρ_{298} values are about 61.9 and 37.7 $\mu\Omega$·cm for the Ba and Sr compounds, respectively. Magnetic susceptibility data for the Ba compound (65.5 mg) and the Sr compound (80.3 mg) were obtained from their ground powders sealed under He in a container described elsewhere.[21] The magnetizations were measured over the range of 2−350 K on a Quantum Design MPMS SQUID magnetometer. The data show almost temperature-independent paramagnetism, $\sim 1.8 \times 10^{-4}$ and $\sim 3.2 \times 10^{-4}$ emu/mol for the Ba and Sr compounds, respectively, over 50−350 K, after corrections for the container and the diamagnetic cores of the atoms. Graphical data for the electrical resistivities and magnetic susceptibilities can be found in the Supporting Information.

Electronic Structure Calculations. To better understand the chemical bonding in the structures and to gain some insight into the roles of magnesium and barium/strontium in the overall bonding, tight-binding electronic structure calculations were performed by both linear muffin-tin orbital (TB-LMTO-ASA)[22] and extended Hückel tight-binding (EHTB)[23] methods. Because all three co-occupied positions have more than 90% Mg, both calculations were carried out on hypothetic compositions of $AeMg_5In_3$ with pure Mg in the three positions. The radii of the Wigner−Seitz (WS) spheres in the former were assigned automatically so that the overlapping potential would be the best possible approximation of the full potential.[24] No interstitial sphere was necessary with an 18% overlap restriction. The WS radii determined by this procedure for all atoms were reasonable: 1.70−1.73 Å for In, 1.56−1.60 Å for Mg, 2.27 Å for Sr, and 2.35 Å for Ba.

Semiempirical EHTB band calculations for $AeMg_5In_3$ composition allowed Mulliken atom population analyses, which provide some guidance as to charge segregation within the particular framework.[25] Mulliken populations for valence orbital occupations were evaluated by integrating over a set of 396 **k** points in the irreducible wedge of the primitive orthorhombic Brillouin zone. The following atomic orbital energies and exponents were employed in the calculations (H_{ii} = orbital energy, eV; ξ = Slater exponent, respectively): In 5s: −12.6, 1.903; 5p: −6.19, 1.677; Mg 3s: −9.0, 1.10; 3p: −4.5, 1.10.[26] The atom parameters for Sr and Ba came from Klem et al.,[27] in which the H_{ii} values for valence d orbitals of Sr and Ba were obtained following Burdett's method for multiplicity corrections to the spectroscopic data for neutral atoms.[28]

Results and Discussion

Crystal Structures. The general view of $BaMg_5In_3$, in Figure 1a, illustrates the 3D Mg−In network, which is constructed from a single, basic building unit, the 21-vertex polyhedron centered by barium, $Ba@Mg_5M_7In_9$ (M = Mg/In), shown in Figure 1b. This polyhedron can be described as a distorted hexagonal prism that sandwiches Ba, plus nine additional atoms in a distorted nonagon that are coplanar with Ba and lie about the waist, that is, an overall 6−9−6 arrangement of planar rings. These lie perpendicular to the

(21) Guloy, A. M.; Corbett, J. D. *Inorg. Chem.* **1996**, *35*, 4669.
(22) van Schilfgarde, M.; Paxton, T. A.; Jepsen, O.; Andersen, O. K.; Krier, G. *Program TB-LMTO*; Max-Plank-Institut für Festkörperforschung: Stuttgart, Germany, 1994.
(23) Ren, J.; Liang, W.; Whangbo, M.-H. *CAESAR for Windows*; Prime-Color Software, Inc.: North Carolina State University: Raleigh, NC, 1998.
(24) Jepsen, O.; Andersen, O. K. *Z. Phys. B* **1995**, *97*, 35.
(25) Lee, C.-S.; Miller, G. J. *J. Am. Chem Soc.* **2000**, *122*, 4937; Lee, C.-S.; Miller, G. *Inorg. Chem.* **2001**, *40*, 338; Li, B.; Corbett, J. D. *Inorg. Chem.* **2004**, *43*, 3582.
(26) Canadell, E.; Eisenstein, O.; Rubio, J. *Organometallics* **1984**, *3*, 759.
(27) Klem, M. T.; Vaughey, J. T.; Harp, J. G.; Corbett, J. D. *Inorg. Chem.* **2001**, *40*, 7020.
(28) Brennan, T. D.; Burdett, J. K. *Inorg. Chem.* **1993**, *32*, 746.

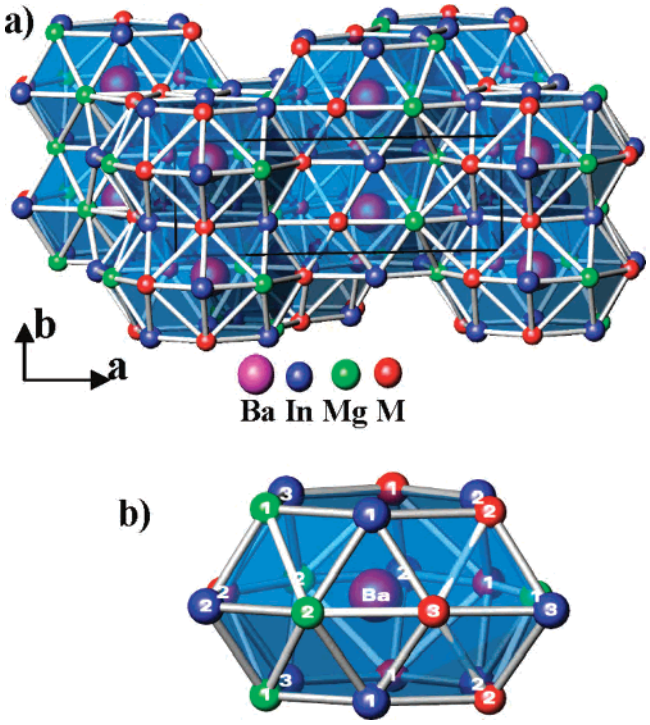

Figure 1. (a) General ~[001] view of $BaMg_{4.8}In_{3.2}$ with a 3D Mg−In network composed of a single basic building unit; (b) 21-vertex polyhedra centered by barium, $Ba@Mg_5M_7In_9$ (M = Mg/In).

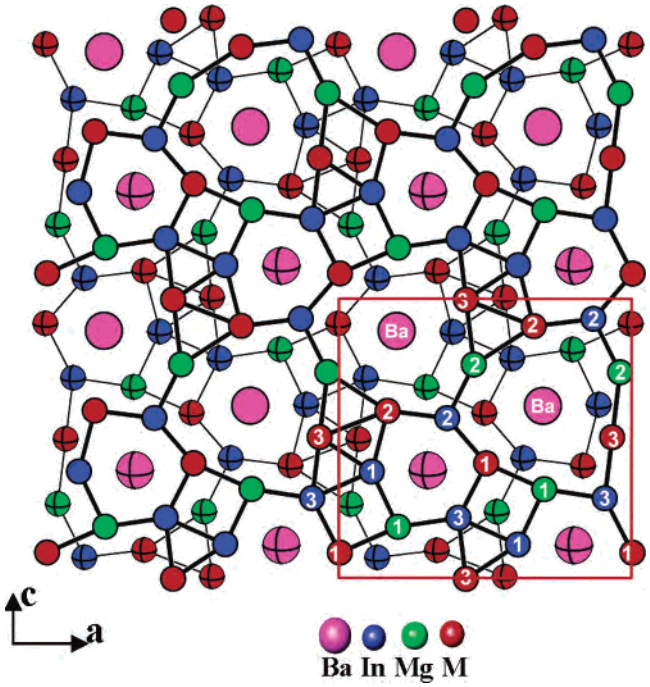

Figure 2. [0−10] view of the crystal structure of $BaMg_5In_3$. The atoms connected by thick and thin lines are at $y = {}^1/_4$ (empty) and $y = {}^3/_4$ (crossed), respectively, and the connections between layers are not shown for clarity. Condensed 6−9−6 polyhedra of Mg/In are centered by Ba (text).

b axis, along which these polyhedra stack by sharing the hexagonal faces. In the *ac* plane, the nine-member ring of each polyhedron shares edges with two other coplanar nine-member rings and with three six-member rings of neighboring polyhedra (displaced by ${}^b/_2$), as shown in Figure 2. (The bonds between layers are not shown for clarity.) No variations in lattice dimensions of samples from different syntheses could be found, in spite of the fractional site occupancies, which suggest that only narrow homogeneity ranges are present.

Some of the overall drive for the formation of such a complex structure can be interpreted in terms of the need to give each Ae cation as many close neighbors as possible from the more anionic Mg−In network. The principle was evidently first put forth for the monoclinic structure of $SrIn_4$,[3] and parallel interpretations have been applied to orthorhombic $BaAu_2Tl_7$[29] and (Ba, Sr)Au_2In_2,[30] both of which occur in the same *Pnma* space group as here. Most of these involve pentagonal prisms about Ae augmented by a coplanar ring of waist atoms, whereas the smaller Mg here allows even higher total coordination, but with an increased structural complexity. The arrangement in Figure 2 can be described in more detail in terms of zigzag chains of coplanar hexagonal prisms along *a* that are in turn stacked along *c* alternately at $b = {}^1/_4$ or ${}^3/_4$. Each Ba thus has six Ba-centered neighboring prisms, two coplanar prisms that share outer rings and define the chains (above), and three in which pairs of the outer nine-ring atoms are inner atoms in neighboring hexagons, and vice versa. This is a common model of augmentation in this kind of structure. The sixth Ba−Ba relationship is at a different level and more complex, without ring sharing, rather, two assemblies that overlap with a step of ${}^b/_2$.

The Mg−In and M−In bond distances have a rather narrow range of 2.901−3.081 Å, suggesting they are dominant within the net. The lengths are comparable to those in $K_3Mg_{20}In_{14}$ (2.944−3.250 Å), a 3D Mg−In network mainly formed from K-centered, 22-vertex polyhedra, $K@Mg_{12}In_{10}$.[13] In the present case, there are only single examples of In−In and Mg−Mg contacts without considering the mixing atom sites: In1−In3 bridging two 21-vertex polyhedra (Figure 2) and Mg1−Mg2 within the 21-vertex polyhedron (Figure 1b). The latter (3.529 and 3.467 Å) are somewhat longer than those formed in $Mg_2Cu_6Ga_5$ (3.00 Å)[7] and $Mg_{35}Cu_{24}Ga_{53}$ (3.16−3.32 Å),[8] but they still represent bonding interactions, as indicated later.

The ideal $BaMg_5In_3$ would be isotypic with that of YCo_5P_3,[31] which can likewise be described in terms of a single basic building unit: 21-vertex polyhedra centered by yttrium, $Y@Co_{12}P_9$, with comparable polyhedral sharing. However, the bridges between polyhedra are different because the reasonable In1−In3 bond (3.19 Å) bridging two polyhedra here (Figure 2) becomes d(P−P) = 3.26 Å in YCo_5P_3, too long to be significant. It is interesting to notice that the present structure is isotypic with that of $Ca_2In_4Au_3$[32] but with an inverse atom distribution in the anion. In this case, In occupies five of the six Mg or Mg/In positions, the second Ca2 lying in the sixth (Mg2) position, whereas Au occurs in what are the three In sites in $AeMg_5In_3$. The contrast in atom distribution amounts to a switch of the most negative atom in each case, viz., $Ca(CaIn_4)Au_3$ versus (Sr,Ba)$(Mg_5)In_3$. Simple explanations of the greatly altered

(29) Liu, S.; Corbett, J. D. *Inorg. Chem.* **2004**, *43*, 2471.
(30) Dai, J. C.; Corbett, J. D. Submitted for publication.
(31) Meisen, U.; Jeitschko, W. *J. Less-Common Met.* **1984**, *102*, 127.

bonding roles in terms of standard metallic radii or electronegativities do not seem to apply, but the nearest-neighbor environments about Ae are sensible. That is, the more negative Au and In atoms in the two phases are closer to the formal cations Ca versus Sr, Ba, respectively, whereas In and Mg are the more distant. Perhaps then the cation sizes are controlling, following the earlier proposition that the difference in structures between isotypic $Ca_2In_4Au_3$ and $Sr_2(Pt,Au)_3In_4$ ($Hf_2Co_4P_3$-type, *P*-62*m*) originates with cation size.[32] However, more convincing arguments or representations arise from bond strength and site charge calculations, as follow.

Electronic Structure and Chemical Bonding. LMTO calculational results for $BaMg_5In_3$ and $SrMg_5In_3$ are very similar, and principally only the former will be used to rationalize the chemical bonding. As shown in the density of states for the idealized $BaMg_5In_3$ in Figure 3a, the Fermi level marked for $BaMg_{4.787(3)}In_{3.213}$, 84.84 e^-, intersects a finite DOS, in agreement with the observed metallic property according to electrical resistivity measurement results (Supporting Information). The minimum DOS at a noteworthy pseudogap corresponds to 85.6 valence electrons, 0.8 e^- higher, which may reflect some additional site preference energies[25] for the electron-poorer Mg. However, E_F for the fully stoichiometric $BaMg_5In_3$ would lie 0.06 eV even lower, clearly suggesting an energetic reason for the observed In substitution. The DOS contributions of Ba, Mg, and In orbitals at E_F are about 19, 38, and 43%, respectively. Taking into account the number of each atom in the unit cell, Ba 5d constitutes the largest contribution over the whole range, but here in a largely nonbonding role. (Appreciable mixing of empty d orbitals of the alkaline-earth elements with post-transition p states appears to be a common theme.[33])

To check the interactions between atom types, crystal orbital Hamilton population analyses (−COHP) were also evaluated, Figure 3b. At the Fermi level, both In−In and Mg−Mg bonds are effectively optimized, whereas the In−Mg data show some bonding character still remains. Note that the frequency of In−Mg bonds is more than ten times that of In−In, one reason for their relative large −COHP values. To quantify the interaction between atoms, integrated crystal overlap Hamiltonian populations (−ICOHP) analyses were also determined, these being better analogues of relative bond strengths than Mulliken overlap populations (MOPs) from extended Hückel methods. Those for In−Mg and In−M are the largest, all in the range of 1.10−1.28 eV/bond, indicating very substantial In−Mg bonding interactions, from which small positive charges for Mg might be expected. The In−Mg value is significantly higher than that for In−Ca2 (0.5 eV/bond), the network Ca in the isotypic $Ca_2In_4Au_3$[32] as we calculated by the same method. In other words, the Ca2 versus Mg2 atoms show markedly different bonding characters with their neighbors even though they occupy the same crystallographic site. However, the −ICOHP values for In−Sr in $SrMg_5In_3$ are about 0.4 eV/bond, similar to those for In−Ca2 in $Ca_2In_4Au_3$.

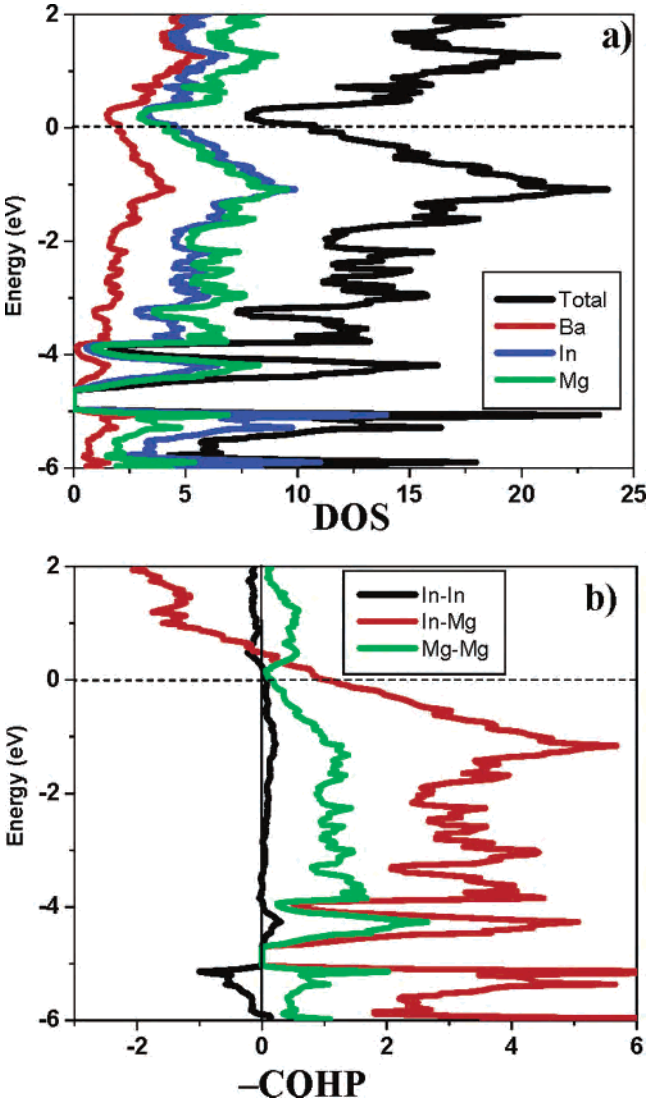

Figure 3. TB−LMTO−ASA electronic structure calculation results for $BaMg_5In_3$. (a) Total DOS (black) and partial DOS curves: indium (blue); magnesium (green); barium (red). (b) −COHP curves for three different interactions: In−In(black); In−Mg (red); and Mg−Mg (green). (The last two are minor in frequency.) The dotted lines denote the Fermi level for the observed composition $BaMg_{4.787}In_{3.213}$.

Table 4. Estimated Charge Contrasts between Isotypic $Sr(Mg_5)In_3$ and $Ca(CaIn_4)Au_3$

$SrMg_5In_3$									
sites	Sr	In1	In2	In3	M1	M2	M3	Mg1	Mg2
charge	+1.36	−0.78	−1.20	−0.86	+0.19	+0.26	+0.43	+0.24	+0.35
$Ca(CaIn_4)Au_3$									
sites	Ca1	Au1	Au3	Au2	In1	In3	In4	In2	Ca2
charge	+1.37	−1.30	−1.07	−1.23	+0.16	+0.18	+0.29	+0.23	+1.36

The Mulliken population analyses for the separate atom types in $SrMg_5In_3$ and in $Ca_2In_4Au_3$ from EHTB calculations are listed in Table 4. The chemical contrast between the two or, better, the parallel between approximate charges on atoms in equivalent positions is manifest. The more negative or electron-withdrawing atoms are In in $SrMg_5In_3$ but Au in $Ca_2In_4Au_3$, whereas the more nearly neutral atoms (+0.16 to +0.43) are the five connecting Mg (M) positions in $SrMg_5$-

(32) Hoffmann, R.-D.; Poettgen, R. *Z. Anorg. Allg. Chem.* **1999**, *625*, 994.
(33) Mudring, A.-V.; Corbett, J. D. *J. Am. Chem. Soc.* **2004**, *126*, 5277.

In_3 versus In1−In4 in $Ca_2In_4Au_3$, Ca2 in the former Mg2 site standing out as a cation (+∼1.36). The results are not sufficiently accurate to distinguish Mg sites from M sites, though.

The estimated Mg charges in the present compounds are similar to those for Mg in $K_3Mg_{20}In_{14}$, which also has dominant Mg−In bonding,[13] but they are notably smaller than those similarly estimated for Mg in Mg_2Zn_{11} (+1.49) and $Mg_2Cu_6Ga_5$ (+1.48),[13] in which Mg is the strongest electron donor and appears to act more as a spacer. The estimated charges for Ba and Sr here are +1.82 and +1.23, respectively. Even allowing for the limitations of these Mulliken analyses, the results clearly show that Mg atoms have an important participation in the covalent bonding of the present structure, but Ba and Sr atoms do not. Notice the large charge differences between Ca2 (+1.36) and Mg2 (+0.29) in the isotypic $Ca_2In_4Au_3$ and $AeMg_5In_3$ even though they occupy the same crystallographic site.

Conclusions

In alkali-metal−Mg−In systems, Mg preferentially occurs in the anionic clusters with In, as in $K_3Mg_{20}In_{14}$, $K_{34}In_{91.05(9)}Mg_{13.95}$, and $Rb_{14}Mg_{4.5}In_{25.5}$, thus behaving somewhat similar to Li in $K_{34}In_{92.30(7)}Li_{12.70(7)}$ and $K_{14}Na_{20}In_{91.82(8)}Li_{13.18(8)}$.[12] Here, the metallic compounds $AeMg_5In_3$ (Ae = Ba, Sr) also exhibit substantial Mg participation in the overall bonding, whereas Ba and Sr are encapsulated in the Mg−In polyhedron and act more as electron donors. Furthermore, preferred charge distributions in the anionic net structure allow a novel role reversal in atom sites, as seen here for $AeMg_5In_3$ versus $Ca_2In_4Au_3$. Similar effects have been noted in diverse icosahedral quasi-crystal approximate structures as well.[35]

Acknowledgment. We are indebted to S. Budko for the magnetic susceptibility data.

Supporting Information Available: Refinement parameters for $BaMg_{4.787(3)}In_{3.213}$ and $SrMg_{4.837(2)}In_{3.163}$ in cif format and resistivity and magnetic susceptibility data for both compounds. This material is available free of charge via the Internet at http://pubs.acs.org.

IC0621289

(34) Pauling, L. *The Nature of the Chemical Bond*, 3rd ed.; Cornell Univ., Ithica, N.Y.; 1960.
(35) Lin, Q.; Corbett, J. D. *Proc. Nat. Acad. Sci. U.S.A.* **2006**, *103*, 13589.